LED-Based Temperature Sensor

Fahimeh Dehkhoda, Ahmed Soltan, Nikhil Ponon, Anthony O'Neill and Patrick Degenaar
School of Engineering, Newcastle University, Newcastle upon Tyne NE1 7RU, UK

Email: {fahimeh.dehkhoda, ahmed.abd-el-aal, nikhil.ponon, anthony.oneill, patrick.degenaar}@newcastle.ac.uk

***Abstract*—This work presents a method to determine the surface temperature of micro-photonic medical implants like LEDs. Our inventive step is to use the photonic emitter (LED) employed in an implantable device as its own sensor and develop readout circuitry to determine the surface temperature of the device. There are two primary classes of applications where micro-photonics could be used in implantable devices; opto-electrophysiology, and fluorescence sensing. In such scenarios, intense light needs to be delivered to the target. As blue wavelengths are scattered strongly in tissue, such delivery needs to be either via optic fibres, two-photon approaches, or through local emitters. In the latter case, as light emitters generate heat, there is the potential for probe surfaces to exceed the 2ºC regulatory. However, currently, there are no convenient mechanisms to monitor this in-situ. This paper, therefore, presents a method to measure the device surface temperature. The proposed sensing system has been designed in 0.35 µm CMOS technology which mainly includes a second generation current conveyor and an amplifier to bias LED and measured the temperature sensitive parameter.**

Keywords— temperature sensor; LED; surface temperature; optogenetics

I. INTRODUCTION

Implantable devices are becoming increasingly important in clinical practice. Biosensors, pacemakers and prosthetics such as visual prosthesis [1, 2] may all utilise optoelectronics. These can be classified into two primary applications: opto-electrophysiology [3] and fluorescence sensing [4]. The former allows control and recording of electrical activity in tissue. The latter can be used to explore chemical changes in cells or their environment. All approaches in optogenetics require moderate to high-intensity irradiation [5]. The requirement for light delivery in close proximity to the stimulus target can be achieved by one of two methods: Light can be generated at some distance and then guided to the local position using optical confinement (e.g. optic fibre or waveguide) until the point of delivery [6]. Alternatively, light can be produced locally on a penetrating or otherwise implantable device incorporating a micro-photonic element [7]. The latter method is able to multiplex multiple electronic outputs leading to a small cable. As the light required for optogenetics is primarily blue and must be high radiance, Gallium Nitride light emitting diodes (LEDs) are the primary technology. High radiance micro-photonics for neural stimulation have been successfully demonstrated in planar high radiance arrays by Soltan et al. [8] and Berlinguer-Palmini et al. [9].

This work is sponsored by the Engineering and Physical Research Council and the Wellcome Trust (www.cando.ac.uk).

In the case of micro-photonic generation close to the target, the key issue is the formation of localised hot spots close to the biomedical device surface. It was shown by Stujenske [10] in 2015 that high radiance light absorption from optic fibre emission can cause localised tissue heating. If the emission source is micro-photonic element, then there is additional potential for heating. McAlinden et al. in 2013 proposed from modelling that there could additionally be a few degrees in temperature rise depending on how the micro-photonic element is driven [11]. The current literature is not entirely clear on what long term effects could result from such temperature increase.

Different on-chip temperature sensors have been used to monitor human health for diseases diagnosis and treatment. The adaptive multi-sensor CMOS system proposed by Huang et al. [12] comprises different on-chip sensors including a temperature sensor which is using a pn junction to sense the body temperature. The low-cost CMOS thermal sensor chip for biomedical application presented by Lee et al. is also employing a pn junction as temperature sensing element [13]. The downside of using additional sensors is that they take additional surface space and need additional address architectures which may present difficulties to integration. Furthermore, it increases the complexity and thus cost of fabrication. Separate sensors for temperature sensing may cause a danger that failure in the sensor may provide inaccurate readings. By utilising the employed micro-photonic emitter in an implantable device as its own sensor, the continued functionality of the device is intrinsically linked to its self-diagnosis.

In this work, LED as microphotonic emitter is presented as its own sensor in medical devices where a readout circuitry is developed to bias and measure the temperature sensitive parameter (TSP). Fig. 1 shows a single penetrating active opto-electrode (optrode) and its general construction with inbuilt stimulation, recording circuits with a control logic unit [14]. Stimulation sites with micro/mini-LEDs for optical emission and electrical recording sites with microelectrodes are placed along the shaft. The main issue here is the localized heating effects at the device surface caused by the shining LEDs. The proposed sensor has been designed using 0.35 µm standard CMOS technology which operates in antiphase with optical stimulation and senses the LED reverse current as temperature sensitive parameter. As the surface temperature of a probe heats up, the junction temperature will also increase. The charge carrier generation in diodes is temperature dependent. As such, if the junction temperature (which is a function of surface temperature) increases, there will be a corresponding change in the LED carrier generation.

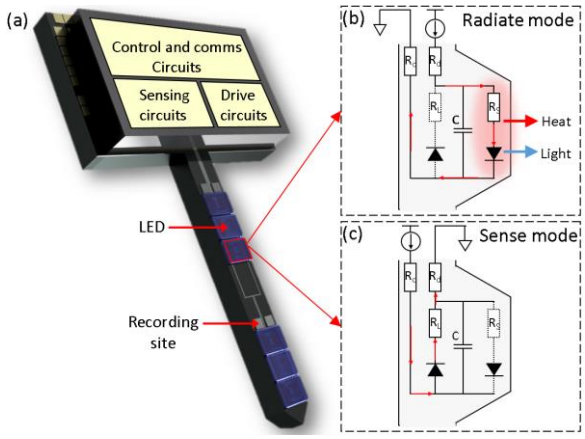

Fig. 1 an illustration of optrode with LED and recording site on the shaft and driving and sensing circuits on the head (a) top view, (b) cross-section view showing forward biased LED and heat generation, (c) cross-section view showing reverse biased LED in a thermal sensing mode.

In forward bias, the LED current exponentially increases with voltage, and thus small changes in temperature are not perceptible. However, in reverse bias, currents are dominated by leakage processes across the diode. In this case, the effect of voltage is still an order of magnitude greater than the effect of temperature change, but if current can be measured at a very stable voltage, then junction temperature can be ascertained. The paper structure is as follows: Section II describes LEDs as a temperature sensor. The microelectronic structure of the sensor is explained in Section III. Section IV provides the experimental results, and Section V concludes the paper.

II. LEDs as Temperature Sensor

The operation of light emitting diodes is temperature dependant in both forward and reverse bias. However, the dynamic range of such effects reduces with increasing current, whereas large currents are required for light emission. As such, to utilise the LED to measure its own temperature, it is best operated at low currents. This is perhaps best performed in reverse bias where the variance of current with applied voltage is minimum.

Jung et al. [15] presented leakage current analysis of Gallium Nitride light emitting diodes in 2015. They showed that there were effectively 4 phases in the general conduction mechanism: Shunt resistance R_{Sh}, parasitic diode, main diode, and sheet resistance R_S. The shunt resistance, which is responsible for the leakage has been presented as having two primary mechanisms: variable range hopping (<300K), and thermally-assisted multi-step tunnelling (>300K). This description was also supported independently by Shan et al [16]. For implantable systems, the base temperature would be expected to be 310K (i.e. 37^{O}C) which is therefore in the latter range. From the perspective of sensing, this means that reverse leakage current is strongly and nonlinearly dependent on both applied field and temperature. As such, to measure temperature accurately, the applied reverse voltage must be kept constant. Furthermore, the temperature dependence of the LED current is effectively dependent on the temperature quantum well junction. In contrast, from the perspective of the sensor, it is the temperature of the surface of the probe which is of interest.

III. Microelectronic Architecture

A key issue with utilising the LED as a temperature sensor is that the current changes with both voltage and temperature. Therefore, a compact microcircuit can be developed to sense the reverse current at a very stable voltage – i.e. stable with temperature, drift, and power supply fluctuations. An optimal circuit for achieving this is a second generation current conveyor (CCII). It can be used to provide a precise bias voltage at the input (X) while receiving current using the same input terminal [17]. The output of the current conveyor can then be transmitted to a transconductance amplifier. The subsequent output voltage can then be transferred to an analog to digital converter for digital transmission and analysis.

Fig. 2(a) depicts a block diagram of the developed microelectronic circuits including the designed switches in a H-bridge structure connected to the designed CCII and transimpedance amplifier (TIA). External 8 bit digital to analog converter (DAC) and 8 bit analog to digital converter (ADC) are employed to provide the required pulse width modulation (PWM) at the input and digitise the output. The CCII receives the bias voltage at the Y terminal and copies the voltage to X terminal to bias the LED. V_X follows V_Y and the output current follows the input current (i.e. LED's reverse current) received at X. The designed TIA converts and amplifies the output current of CCII with a gain of 5×10^5 V/A.

The sensor operates in antiphase with LED light emission i.e. the first phase is light emission using forward biased LED through S1 switches while the intensity is controlled using PWM. The second phase is temperature sensing with reverse biased LED through S_2 switches. The functionality of the sensor is explored by switching the LED from light emission to sensing phase inside an isolated dark box and using a continuous pulse. The generated heat after pulsing LED was collected using IR camera as surface temperature. Fig. 2(b) shows a timing diagram of light emission (PW_1) and temperature sensing (PW_2) phases. The layout of the designed temperature sensing system including the switches and control logic, biasing circuit, CCII and TIA are shown in Fig. 3.

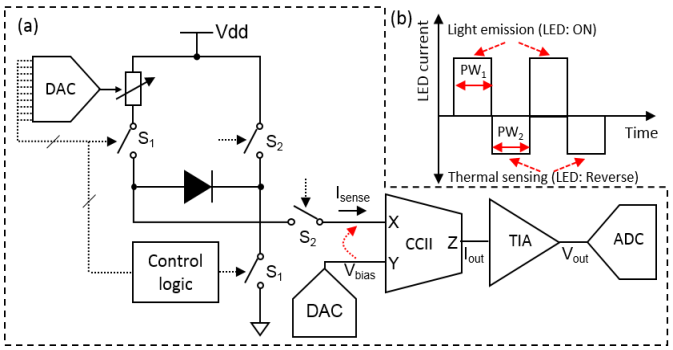

Fig. 2 (a) Block diagram of the proposed temperature sensing system with light illumination phase through S1 and thermal sensing phase through S2. DAC provides the bias voltage for LED through CCII which receives the reverse current. A TIA converts and amplifies the current, (b) a timing diagram of the LED bias current in two phases.

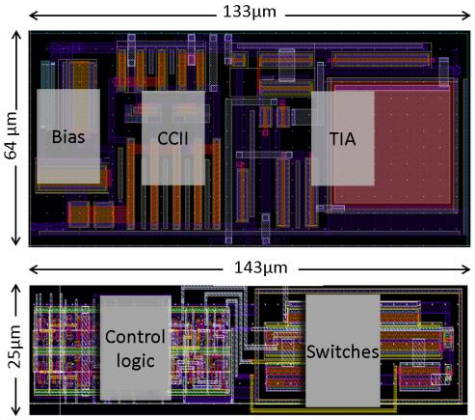

Fig. 3 layout of the designed temperature sensing system including the switches and their control logic, biasing circuit, CCII and TIA

IV. EXPERIMENTAL RESULTS

The implemented system clamps a reverse bias voltage with a high degree of accuracy across the LED in order to differentiate between temperature variation and voltage variation. The voltage stability is within ±5% of a target bias voltage. Temperature change can be accurately determined despite variations in power supply noise. A calibration process should be performed using the current-voltage-temperatures characteristic of the utilised LEDs in reverse bias to attain the surface temperature and current dependency of LEDs. Also, different experiments are carried out to explore the relation between the junction and surface temperatures.

We have experimentally explored the temperature dependency of the reverse current in mini-LEDs. Fig. 4(a) shows the experimental setup to characterise the LEDs inside an isolated dark box which guarantees that the measured current is only due to the temperature change. The box is also temperature isolated to ensure the accuracy of the measured temperature. A hot plate is also placed under the LED to change the temperature to characterise the LED. Temperature change was captured and recorded by an IR Optris PI camera and its interface software, respectively.

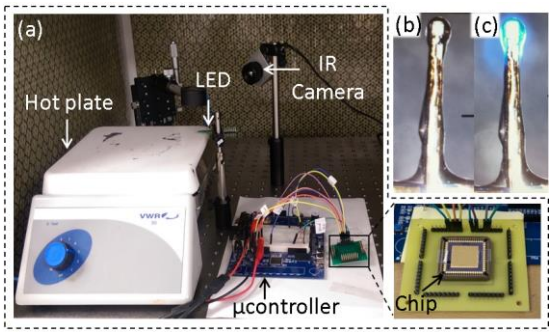

Fig. 4 (a) experimental setup inside an isolated dark box to characterise the LED and sensor (b)-(c) encapsulated mini-LED (off and on) mounted on a silicon shank representing a typically penetrating probe for the brain cortex.

CREE DA2432 mini-LEDs are used to develop an exemplar probe to determine their capability of measuring temperature in systems similar to the final embodiment. Probes were developed on silicon shafts which were 4mm long, 300µm wide and 200 um thick (Fig. 4(b)-(c)). Titanium/Gold/Titanium metal tracks were deposited at a thickness of 20/200/20 nm and patterned. The metal tracks had a width of 30 um. Top Titanium on the bond pads were later removed and the Gold surface exposed. The mini-LEDs were bonded on using silver epoxy (RS Pro Silver Vial Epoxy Conductive Adhesive) with a pick and place machine (FINEPLACER® lambda from Finetech). The LEDs had a size of 240×320 $(\mu m)^2$ and thickness of 140µm.Transparent silicone (NuSil MED-1000) was used to dip coat and encapsulate the LEDs. The encapsulated silicone had an average thickness of 50µm.

Fig. 5 (a) shows the I-V characteristics of a reverse biased mini-LED at different temperatures. The reverse current dependency to voltage change is more than its dependency to temperature variations. This means the LED needs to be interrogated at a fixed reverse bias which does not deviate in time or due to noise. Fig. 5 (b) shows the absolute value of reverse current versus temperature in two different reverse bias voltages. The LED current is measured in a fixed bias voltage while the temperature is changing using hotplate. There is a good linearity between reverse current and temperature which means the reverse current can be used as TSP.

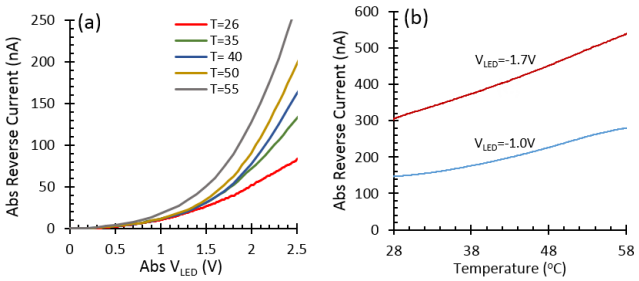

Fig. 5 (a) the absolute value of reverse current versus absolute voltage of a mini-LED in different temperatures, (b) absolute value of reverse current versus temperature in two different reverse bias voltages -1.7V and -1.0V.

Different experiments are conducted to achieve the junction temperature variation (ΔT_J) and surface temperature variation (ΔT_S) of mini-LEDs connected to the sensing circuit. To explore this, two different experiments are conducted. First experiment includes the reverse biased LED on a hot-plate inside the isolated dark box. The output current is measured while temperature is increasing using the hotplate. Fig. 6 (a) shows the output current change versus ΔT_J. In the second experiment, a long pulse is applied to the LED and the output current and ΔT_S are measured in sensing phase. Fig. 6(b) shows the output current change versus ΔT_S when a 2.5mA pulse with 3msec pulse width is applied to the LED for a few minutes to increase the surface temperature. The results clearly show a linear relationship between current and temperature. Fig. 6(c) shows the ΔT_S versus ΔT_J derived using the conducted experiments. Fig. 6(e) shows the sensor output voltage and current versus ΔT_S. For this experiment, a 7.5 mA pulse with 3msec pulse width is applied to the LED for a few minutes. During illumination phase, the surface temperature increases about 10 ºC and the LED reverse current and sensor output voltage change. As shown in the figure, the safe range of temperature rise is up to 2ºC as more temperature rise can cause neural damages. The specifications of the designed temperature sensing circuit are listed in Table 1 which are based on its application on optrode, the power and area requirements and body temperature range.

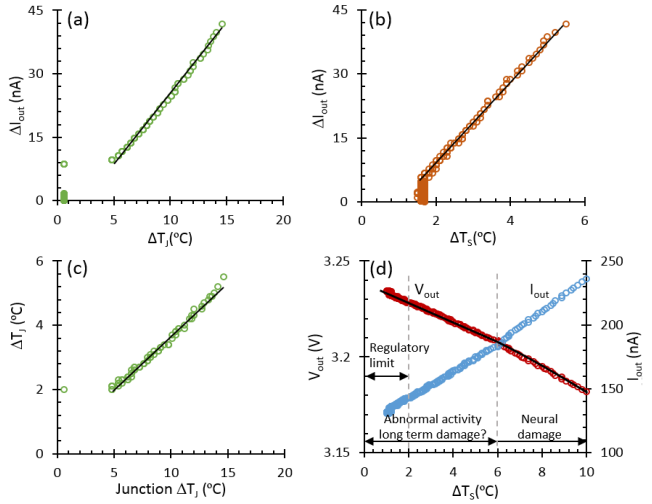

Fig. 6 (a)-(b) measured output current change versus ΔT_J and ΔT_S, respectively when the LED was driven using a 2.5mA pulse with 3msec pulse width (c) ΔT_S versus ΔT_J (d) the sensor output voltage and current versus ΔT_S when the LED was driven for a few minutes using a 7.5mA pulse with 3msec pulse width.

The circuit occupies less area than similar designs as it relies on the employed LED itself as main sensing element. Furthermore, the power consumption of the proposed circuit is less than the designs reported in [12, 13] (Table 2).

Table 1 Design specifications for a mini GaN LED

CMOS Technology (µm)	0.35
Supply voltage (V)	5
Power consumption (Bias+CCII+TIA+Switches) (µW)	260
Overall gain (V/A)	5×10^5
Sensitivity floor (ºC)	0.2
Temperature sensitivity (mV/°C)	5~10
Temperature range (°C)	25~65
Area (Bias+CCII+TIA) (µm^2)	133×64
Area (Switches+Control logic) (µm^2)	143×25

Table 2 Comparison between the proposed work and published works

	[12]	[13]	This work
Temperature range (ºC)	32~42	20~60	25~26
Supply voltage (V)	1.8	1.8/3.3	5
Power consumption (µW)	942	300~2200	260
Technology (µm)	0.35	0.25	0.35
Area (mm^2)	11.25	1	0.012
Sensor device	PN Junc.	PN Junc.	LED

V. Conclusion

A new method of temperature sensing for micro-photonic devices in optogenetics is presented. The proposed systems is based on LED and designed in standard 0.35 µm CMOS technology. The proposed system uses the reverse current of LEDs as TSP to measure the generated heat at the surface of the device. This is to prolong the lifespan of the implants as the increased heat due to LED shining can damage LED bonding and tissue which will affect the device functionality. The designed circuit consists of a second generation current conveyor to bias the LED and receive the reverse current. A high gain amplifier amplifies the signal which represents temperature variations. Different experiments are carried out to achieve the surface temperature of the device where the results show that the reverse current of the LED is a reliable temperature sensitive parameter to detect thermal variations on the LED surface. The proposed method is area efficient as eliminates the area consuming blocks which are usually used for temperature sensors in implantable systems. Also, the danger of failure due to the other devices can be decreased here.

References

[1] J. M. Barret, P. Degenaar and E. Sernagor, "Blockade of pathological retinal ganglion cell hyperactivity improves optogenetically evoked light responses in rd1 mice," *Frontiers in Cellular Neuroscience*, vol. 9, pp. 1-14, 2015.

[2] J. Barrett, R. Berlinguer-Palmini and P. Degenaar, "Optogenetic approaches to retinal prosthesis," *Visual Neuroscience*, vol. 31, no. 4-5, pp. 345-354, 2014.

[3] J. Du, T. J. Blanche, R. R. Harrison, H. A. Lester and S. C. Masmanidis, "Multiplexed, High Density Electrophysiology with Nanofabricated Neural Probes," *PLOS ONE*, vol. 6, no. 10, pp. 1-11, 2001.

[4] A. P. Demchenko, Introduction to Fluorescence Sensing, Springer, 2009.

E. Pastrana, "Optogenetics: controlling cell function with light," *Nature Methods*, vol. 8, pp. 24-25, 2011.

[6] D. R. Sparta, A. M. Stamatakis, J. N. Phillips, N. Hovelso, R. V. Zessen and G. D. Stuber, "Construction of implantable optical fibers for long-term optogenetic manipulation of neural circuits," *Nature Protocol*, vol. 7, no. 1, pp. 12-23, 2012.

[7] H. Cao, L. Gu, S. K. Mohamty and J. C. Chiao, "An Integrated µLED Optrode for Optogenetic Stimulation and Electrical Recording," *IEEE Transactions on Biomedical Engineering*, vol. 60, pp. 225-229, 2013.

[8] A. Soltan, B. McGovern, E. Drakakis, M. Neil, P. Maaskant, M. Akhtar, J. S. Lee and P. Degenaar, "High density, high radiance µLED matrix for optogenetic retinal prostheses and planar neural stimulation," *IEEE Transactions on Biomedical Circuits and Systems*, vol. 11, 2016.

[9] R. Berlinguer-Palmini, R. Narducci, K. Merhan, A. Dilaghi, F. Moroni, A. Masi, T. Scartabelli, E. Landucci, M. Sili, A. Schettini, B. McGovern B and G. Mannaioni, "Arrays of MicroLEDs and Astrocytes: Biological Amplifiers to Optogenetically Modulate Neuronal Networks Reducing Light Requirement," *PLoS One*, vol. 9, no. 9, 2014.

[10] J. M. Stujenske, T. Spellman and J. A. Gordon, "Modeling the Spatiotemporal Dynamics of Light and Heat Propagation for In Vivo Optogenetics," *Cell Reports*, vol. 12, no. 3, pp. 525-534, 2015.

[11] N. McAlinden, D. Massoubre, E. Richardson, E. Gu, S. Sakata, M. D. Dawson and K. Mathieson, "Thermal and Optical Characterization of MicroLED Probes for in vivo Optogenetic Neural Stimulation," *Optics Letters*, pp. 1-4, 2013.

[12] Y. J. Huang, T. H. Tzeng, T. W. Lin and C. W. Huang, "A Self-Powered CMOS Reconfigurable Multi-Sensor," *IEEE Journal of Solid-State Circuits*, vol. 49, no. 4, pp. 851-866, 2014.

[13] H. Y. Lee, C. M. Hsu and C. H. Luo, "CMOS thermal sensing system with simplified circuits and high accuracy for biomedical application Circuits and Systems," in *Proceedings of IEEE International Symposium on Circuits and Systems, ISCAS*, 2006.

[14] F. Dehkhoda, A. Soltan, R. Ramezani, H. Zhao, Y. Liu, T. Constandinou and P. Degenaar, "Smart Optrode for Neural Stimulation and Sensing," in *IEEE Sensors*, 2015.

[15] E. Jung, J. K. Lee, M. S. Kim and H. Kim, "Leakage Current Analysis of GaN-Based Light-Emitting Diodes Using a Parasitic Diode Model," *IEEE TRANSACTIONS ON ELECTRON DEVICES*, vol. 62, 2015.

[16] Q. Shan, D. S. Meyaard, Q. Dai, J. Cho, E. F. Schubert, J. K. Son and C. Sone, "Transport-mechanism analysis of the reverse leakage current in GaInN light-emitting diodes," *applied Physics Letters*, vol. 99, 2011.

[17] S. B. Salem, M. Fakhfakh, D. S. Masmoudi, M. Loulou, P. Loumeau and N. Masmoudi, "A High Performances CMOS CCII and High Frequency Application," *Analog Integrated Circuits and Signal Processing*, vol. 49, pp. 71-78, 2006.